ECOLOGY

Pelagic diatoms communicate through synchronized beacon natural fluorescence signaling

Joan S. Font-Muñoz[1,2]*, Marc Sourisseau[1], Amanda Cohen-Sánchez[3], Idan Tuval[3,4], Gotzon Basterretxea[3]

Communication between conspecific individuals is an essential part of life both in terrestrial and marine realms. Until recently, social behavior in marine phytoplankton was assumed to rely mainly on the secretion of a variety of infochemicals that allowed population-scale collective responses. Here, we demonstrate that pelagic diatoms also use Sun-stimulated fluorescence signals for synchronizing their behavior. These unicellular microorganisms, playing a key biogeochemical role in the ocean, use photoreceptor proteins and red–far-red fluorescent radiation to communicate. A characteristic beaconing signal is generated by rhythmic organelle displacement within the cell cytoplasm, triggering coordinated population behavior. These light-based communication networks could critically determine major facets of diatom ecology and fitness and regulate the dynamics of larger-scale ocean processes.

INTRODUCTION

Social behaviors, defined as interactions between members of the same species, constitute a universal feature of organisms ranging from tiny bacteria to large marine mammals. Becoming member of an organized group has potential positive consequences in the adaptation of an individual to the environment and to the effectiveness of the interactions with other organisms (*1*). Collective and cooperative activities provide increased mating opportunities, improved foraging efficiency, lower predation and infection risk, and reduced energetic costs (*2*). The central principle is that simple repeated interactions between individuals, with or without any purposefulness of the consequences, can produce complex adaptive patterns at the group level (*3*). From these collective behaviors emerge, at higher organizational levels, properties and patterns that can determine the functioning of whole ecological frameworks.

In the marine realm, the importance of socialization has been largely attributed to the more evolved macroscopic metazoans displaying evident communication and cooperative behavior. There are many examples of such social patterns, including fish schooling, crustacean and sea cucumber reproduction, or synchronous spawning of corals (*4*–*6*). However, mounting evidence shows that social conduct is even present in more primitive microorganisms with seemingly more erratic behavior, such as phytoplankton and bacteria, constituting a fundamental aspect of their life (*7*–*10*). Socialization (i.e., a collective activity) would allow microorganisms to behave as multicellular organisms and to obtain benefits that would be unattainable to them as individuals (*11*).

Social behavior is mediated by some sort of characteristic communication mechanism through which individuals coordinate activities. Visually mediated allelomimesis, acoustic and electromagnetic signals, and the release of chemical substances are common information exchange mechanisms in the sea. In the absence of a complex eye or a developed sound-sensing organ, cell-to-cell communication and group organization in marine microbial organisms are thought to be primarily accomplished through the release of small diffusible signal molecules called autoinducers, which trigger cell responses to chemical gradients (*12*–*14*). The information supplied by these biocompounds is critical for synchronizing a variety of activities, including directing communication, mate finding, inducing defenses, modifying behavior, and activating autocatalytic programmed cell death (*15*–*20*). An alternative to chemical communication is the emission and redirection of light by distinct optical mechanisms (e.g., iridescence, fluorescence, chemiluminiscence, scattering, etc.). These mechanisms are well distributed in marine life (*21*), and for example, some bacteria such as marine vibrios have developed luminescence signals to coordinate their activity (*22*).

Among the microbial organisms inhabiting modern world oceans, diatoms (Bacillariophyta) are ubiquitous and dominant unicellular microalgae with a major trophic and biogeochemical role (*23*). They form the base of marine food webs on which ocean life depends, being responsible of between 20 and 40% of the net primary production in the ocean (*24*). Diatoms are also widely regarded as key drivers of the marine biological carbon pump, being responsible of up to 50% of the organic carbon exported to the ocean interior (*25*, *26*). A distinguishing characteristic of diatoms is that their protoplasm is confined in a transparent biomineralized silica shell, the frustule, constituted by two valves ornamented with nanopores of different dimensions and different geometrical distribution interconnected by a lateral girdle.

The success of pelagic diatoms in contemporary ocean conditions suggests a good degree of adaptation to environmental change. They are able to rapidly detect and respond to light, fluid motion (shear stress), osmotic stress, oxygen variations, temperature and nutrient availability (*25*, *27*–*30*). Besides individual physiological adaptations, some of these behaviors entail sophisticated strategies of collective response to changes in the environment that can be manifested as short-term massive blooms alternated with coordinated cell deaths, sexual reproduction events, and/or collective sinking of the population (*31*). Current understanding of communication processes in marine diatoms suggests that responses to environmental variations are collectively organized by secreting a

[1]IFREMER, French Institute for Sea Research, DYNECO PELAGOS, 29280 Plouzané, France. [2]Université de Brest-UBO/CNRS/IFREMER/IRD, 29238 Brest, France. [3]Mediterranean Institute for Advanced Studies, IMEDEA (UIB-CSIC), Miquel Marques 21, 07190 Esporles, Balearic Islands, Spain. [4]Department of Physics, University of the Balearic Islands, Ctra. Valldemossa Km. 7.5, 07122 Palma, Balearic Islands, Spain.
*Corresponding author. Email: jsfontmu@ifremer.fr

variety of infochemical signals that are perceived and amplified by others, thereby spreading a message throughout the whole population (*32*, *33*). However, in photosynthetic eukaryotes, light is not only necessary for metabolism (photosynthesis) but also provides spatiotemporal information, regulating key biological functions such as cell movement and organized development (*34*, *35*).

Here, we experimentally demonstrate that besides chemical molecules, pelagic diatoms also use light for intercellular communication and to develop social patterns (see fig. S1). We use laser diffractometry (LD) combined with chlorophyll fluorescence and flow cytometry to reveal a collective response of *Pseudo-nitzschia delicatissima* laboratory cultures to environmental light. We observe that under low shear conditions commonly existing in the sea, pennate diatoms manage to orient vertically and re-emit sunlight as modulated chlorophyll fluorescence cues. This distinctive signal is produced by a wobbling cell movement that is achieved by fast periodic reorganization of intracellular organelles. Moreover, individual light emissions are rapidly synchronized (over a minute time scale), identifying a population signature that evidences coordinated behavior. The consequences of unraveling the communication and social behavior of marine diatoms are enormous, ranging from the understanding of how microorganism interactions are driven in the ocean, to advances in the biological drivers of large-scale phytoplankton blooms influencing ocean productivity and carbon sequestration in the sea.

RESULTS AND DISCUSSION

Although generally considered nonmotile organisms in the pelagic environment (they can only glide over surfaces using their raphe), diatoms are indeed endowed with limited ability to move and selectively orient their trajectories. By regulating their buoyancy, some large diatoms can transit to deeper waters in search of higher nutrient availability and actively return to depths where light conditions allow optimal growth. This well-documented vertical migration over diurnal time scales often occurs as a collective response to diverse environmental and physiological cues (*36*).

Here, we report a shorter time scale response consisting of a coordinated cell orientation in the water column and a synchronized cell movement. This behavior is observed when pennate diatoms of the species *P. delicatissima* are exposed to light in low shear conditions typical of the oceanic environment (i.e., $\gamma < 0.1\ s^{-1}$) (*37*, *38*). This previously overlooked photoresponse, which is characterized by a vertical alignment and synchronic wobbling (~30° from the vertical) at frequencies of ~0.01 Hz (104 ± 2 s period), is also observed in the fusiform morphotype of *Phaeodactylum tricornutum* with minor interspecific differences in the wobbling period (90 ± 5 s; see fig. S7). Wobbling is not detected in dead cells exposed to the same experimental conditions (Fig. 1A), thereby revealing that it is an active biological process that cannot be attributed to passive hydrodynamics or technical biases.

We use the cell's aspect ratio *R*, defined as the ratio between the cross-sectional, r_1, and the transapical cell axis, r_2, to identify cell orientation (see the "Laser diffractometry" section in Materials and Methods). As shown in Fig. 1 (A and B), the two-dimensional projection of *R* displays a well-defined limit cycle in phase space characteristic of volumetrically coherent, i.e., population level, periodic wobbling when cells are exposed to ambient light. Vertical alignment and wobbling are manifested shortly after cells are illuminated (80 ± 23 s) and strongly attenuate tenths of seconds after

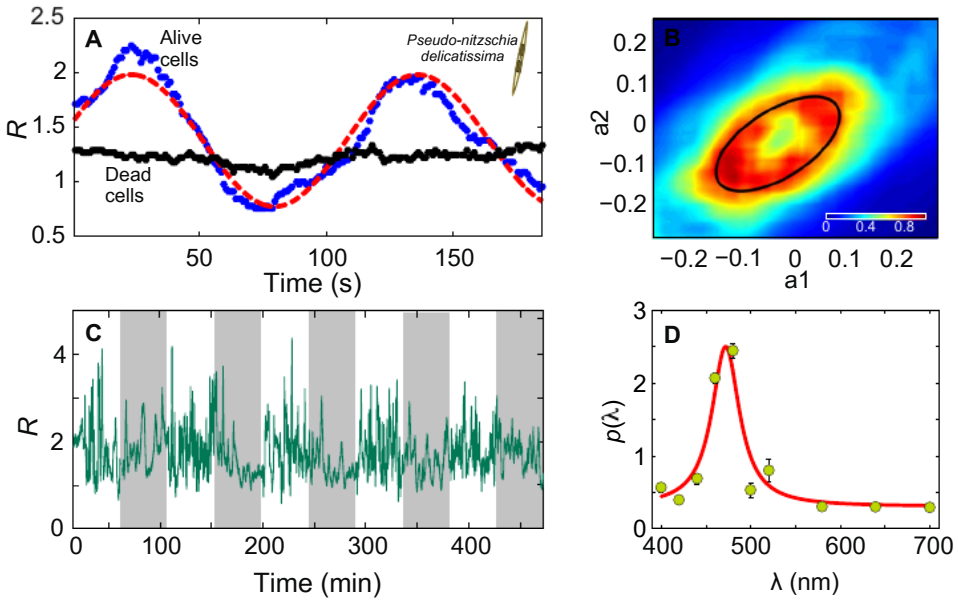

Fig. 1. BL triggers cell wobbling photoresponse. (**A**) Time series of the two-dimensional projection of the of cell's aspect ratio *R* (defined as the ratio between the cross-sectional, r_1, and the transapical cell axis, r_2) for living (blue dots) and dead (black dots) *P. delicatissima* cells and its fit to a sinusoidal function (dashed red line). (**B**) Two-dimensional phase space reconstruction of the temporal dynamics of *R* in steady state (6000 s) for living cells in daylight conditions (the black line highlights the asymptotic limit cycle). (**C**) Temporal evolution of *R* for long time series experiments with living cells, where periods of light and darkness were alternated (white and gray bands, respectively). (**D**) Power spectral density of the temporal evolution of PC1 for spectrophotometry experiments at different wavelengths and fitted Lorentzian function peaking at (450 to 490 nm).

cells experience darkness (Fig. 1C). The spectral characterization of the wobbling photoresponse shows a well-defined maximum for wavelengths in the band λ ~ 450 to 490 nm (Fig. 1D), which is a prevalent waveband that diatoms have adapted to absorb using pigments such as chlorophyll c2, c3, and fucoxanthin (*39*). It is also compatible with other blue light (BL) responses, such as phototropism or chloroplast photorelocation movements (*35*, *40*), that photosynthetic stramenopiles, including diatoms, have acquired during evolution.

Using particle scanning and fluorescence imaging analysis, we also observe that asymmetric chloroplast rearrangements within the cytoplasm are more frequent in illuminated cells. These asymmetric chloroplast configurations favor wobbling movements as cells migrate vertically. Light-induced chloroplast redistribution is observed widely in the plant kingdom, from algae to seed plants (*41*), and the displacements are controlled by dynamic changes in the configuration of actin filaments in the cytoskeleton. Both the contraction and intracellular movement of chloroplasts in diatoms have been previously related to photoinhibition of photosynthesis and diel fluctuations in cellular fluorescence (*42*, *43*). Actin and a small set of actin-related proteins have been also described to be involved in benthic diatom locomotion (*44*–*46*).

In the case of *P. delicatissima*, image analysis reveals that chloroplasts are located at a distance about one-third of the cell length, 35 to 40 μm from the cross-sectional axis. In complete darkness, the chloroplasts tend to remain next to the center of the cell, whereas wider and asymmetric distributions are observed when cells are exposed to BL (Fig. 2, A and B). As shown in Fig. 2C, concomitant changes in amplitude occur that result in significant variations in the position of the cell center of mass (CoM) and, accordingly, cells wobble as vertically displace in an illuminated environment. The sedimentation model of an ellipsoid sinking under low shear conditions and that incorporates the measured displacements reveals a wobbling dynamics that is compatible with our experimental observations (Fig. 2D). In the case of single chloroplast-bearing diatoms (e.g., *P. tricornutum*) any small displacement would also lead to an asymmetric mass distribution within the cytoplasm producing a change in the CoM. This observation suggests that wobbling could be a widespread feature in pennate diatoms.

Wobbling is suppressed when cells are treated with the cytoskeleton motility inhibitor 2,3-butanedione monoxime (BDM), known to alter actomyosin-regulated chloroplasts movements (*40*, *47*–*49*), dampening the limit-cycle oscillations to a rest (fig. S2). Oscillations are recovered after the inhibitor disposal and cells resuspension. Wobbling is also overridden by externally induced mechanical stresses under increased ambient fluid mixing conditions ($\gamma > 4\ s^{-1}$), suggesting the operation of a yet-unknown mechanosensory loop. Repeated periods of agitation of the fluid (100 s) spaced by periods

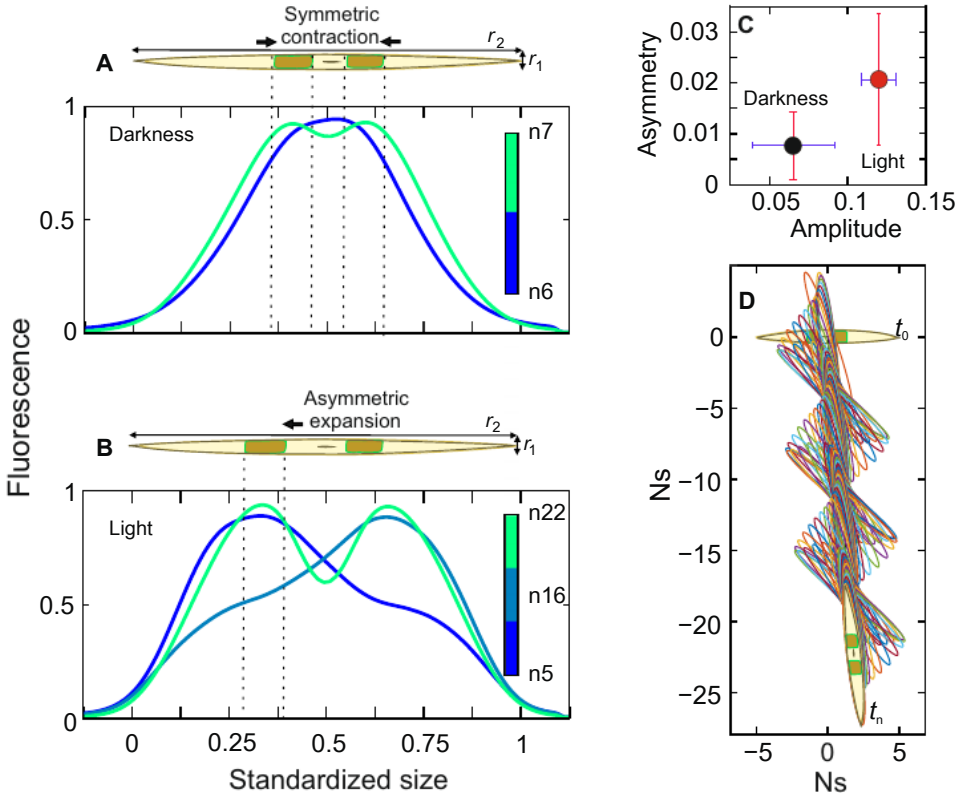

Fig. 2. Active chloroplast rearrangements alter CoM position and induce orientational dynamics in pennate diatoms. Most common chloroplast arrangements of *P. delicatissima* extracted by a self-organizing map (SOM) analysis (neural network of 25 neurons, n1 to n25) (**A**) in the dark and (**B**) when cells are exposed to light. The different colors correspond to the dominant patterns for each light condition (complete analysis is show in fig. S5). (**C**) Comparison of the mean values of asymmetry in the arrangement of chloroplasts and their position with respect to the center of the cell, for cells kept under daylight and dark conditions. (**D**) Simulations of Jeffery's orbits below the critical shear for an ellipsoid with a realistic aspect ratio and a periodic displacement of the CoM.

without agitation (1000s) induce progressive dampening of the oscillations until, eventually, wobbling becomes negligible (fig. S3). Collective cell motility resumes with the same amplitude and period after ~2000s since vigorous agitation of the fluid ceases.

Unexpectedly, BL-induced wobbling can directly modulate cell-emitted luminescence, therefore generating a beaconing red signal. Living diatoms present two main sources of light emission: frustule photoluminescence (*50*, *51*) and autofluorescence from chloroplasts and lipid layers (*52*–*54*). Frustule BL photoluminescence is related to geometrical features of micro- and nanostructures and their refractive index contrast with respect to the surrounding environment (*50*, *55*). The chlorophyll autofluorescence results from part of the absorbed energy from the more penetrating bands (e.g., blue-green) that is released back to the environment in the red–far-red bands (*56*, *57*). It represents only a small fraction of all excitation energy captured by pigments (2 to 5%) (*58*), as energy is efficiently channeled into charge separation (*59*, *60*). At in vivo temperatures, the energy dissipated as light is mostly emitted as fluorescence centered on PSII chlorophyll-a emission band (~680 to 700 nm). These spectral characteristics shape an optical fingerprint unique to photosynthetic organisms (*61*). Furthermore, the distinct optical transmission properties of gridle and valves in the diatoms strongly vary with both wavelength and light incidence angle (*62*). Hence, as cells wobble with respect to the vertical, the emitted chlorophyll fluorescence signal in any arbitrary direction is modulated by the frustule orientation. This results in a perceptible time modulation of the emitted signal at the frequency of cell wobbling (fig. S4).

Intrigued by the effect that this modulated red light signal might have in the dynamics of neighboring cells, its potential role in cell-to-cell communication was further explored. For successful communication, cells must simultaneously act as transmitters and receptors of the transmitted signal. The receptor capacity is in agreement with the observations that organisms (phototrophs or not) present several photosensoring proteins (photoreceptors) that allow them to perceive light signal, adapt, and regulate diverse cellular processes under different light intensities and qualities.

Because of the spectral properties of the underwater light field, BL photoreceptors are expected to be crucial for controlling the life of marine organisms. Some BL photoreceptors (cryptochrome and aureochrome) are thus present in these organisms (*63*). Cryptochromes are related with functions involving DNA repair, circadian rhythm, and photoreception (*64*), whereas aureochromes in diatoms could be involved in BL-induced photoacclimation (*65*). The fact that infrared and red wavelengths are readily absorbed in the water column has led to the common assumption that aquatic organisms sense and adapt to penetrative blue/green light wavelengths but show little or no response to the more attenuated red–far-red wavelengths (*66*). However, red light is transmitted through diatom valves with more efficiency than other spectral bands, and diatoms have red light photoceptors of the phytochrome superfamily (*67*). Not all plastid-bearing eukaryotes encode phytochromes; notably, the Haptophyta, red algae (Rhodophyta), and green algae (Chlorophyta) lack phytochrome genes, but phytochromes present in marine diatoms are functional with several genes being activated by both red and far-red light (*68*, *69*). Last, it has been speculated in previous work that they could play a role in surface detection during algal blooms, as a chloroplast activity sensor deeper down the water column or as a neighbor sensor (*57*, *66*, *70*). The latter would allow diatoms to perceive and potentially respond to the autofluorescence of neighboring cells, especially at subsurface levels of the water column were background red light is negligible.

To highlight potential cell-to-cell communication leading to synchronization, we exposed *P. delicatissima* cells to pulsed red light, mimicking a beaconing signal emitted by neighboring congeners. As illustrated in Fig. 3 (A and B), stimulation with pulsed red light in the frequency of diatom wobbling (~0.01 Hz) progressively entrains cell wobbling and a synchronized response of the population is effective (with a magnitude-squared coherence >0.8) after a short transient after activation of the stimulus (~400 s).

A theoretical framework for understanding this frequency entrainment is offered by the theory of weakly coupled oscillators, which describes under which conditions interacting (coupled) oscillators synchronize (*71*). The ability of coupled oscillators to synchronize is controlled by two opponent forces: their detuning (i.e., difference in intrinsic frequency) and their coupling strength (here, through light intensity). The region in the two-dimensional parameter space of coupling strength and detuning within which synchronization occurs is called the "Arnold tongue." For conditions within the Arnold tongue, the oscillators converge on a common emergent frequency. Within the Arnold tongue, the initial (intrinsic) frequency difference between the oscillators is replaced by a consistent phase difference. Outside the Arnold tongue, intrinsic frequency differences are maintained, precluding a consistent phase relationship (i.e., phase precession instead of synchronization).

We illustrate how frequency entrainment between diatom wobbling (at frequencies Ω) and red light modulation (at frequencies ω) occurs in Fig. 3 (C to E). For a sufficiently small difference in intrinsic frequency $\Delta\omega$ (purple dots and curves in the panels) at the chosen coupling strength (a parameter range falling within the Arnold tongue), the wobbling signal synchronize at the common frequency of the driving signal (red light). This is demonstrated by the overlapping power spectra of both signals (Fig. 3D). If the detuning is either increased or decreased while keeping the coupling constant, then conditions falling outside the Arnold tongue region are created and the two signals do not synchronize but, instead, oscillate at different frequencies. Figure 3C shows a comparison of the intrinsic frequency difference in the absence of coupling (dashed line) and its emergent frequency when coupled. This displays a nonlinear relation whereby frequency is constant within the range of the Arnold tongue.

Cooperation and collective phenomena affect organism fitness and adaptation to the environment. Conspecific communication, which is fundamental for cooperative responses, constitutes an essential factor shaping natural ecosystems. However, communication in marine microorganisms may be more complex than previously envisaged. At a close distance, notably when cells aggregate or form chains, chlorophyll autofluorescence overcomes the background radiation in the red–far-red band and its modulation becomes an effective (fast and inexpensive) signaling strategy. Red light has been already proven to induce collective responses in diatoms including variations in their sinking rate and the triggering of sexual reproduction (*72*, *73*). Here, we demonstrate that the modulated autofluorescence signal produced by cell wobbling can be detected by neighboring cells and induce synchronized responses. Moreover, we have been able to induce such responses by interrogating cells with pulsed red light in the frequency band generated by cell wobbling. To the best of our knowledge, this is the first report of autotrophic plankton communication through cell luminescence in this spectral band.

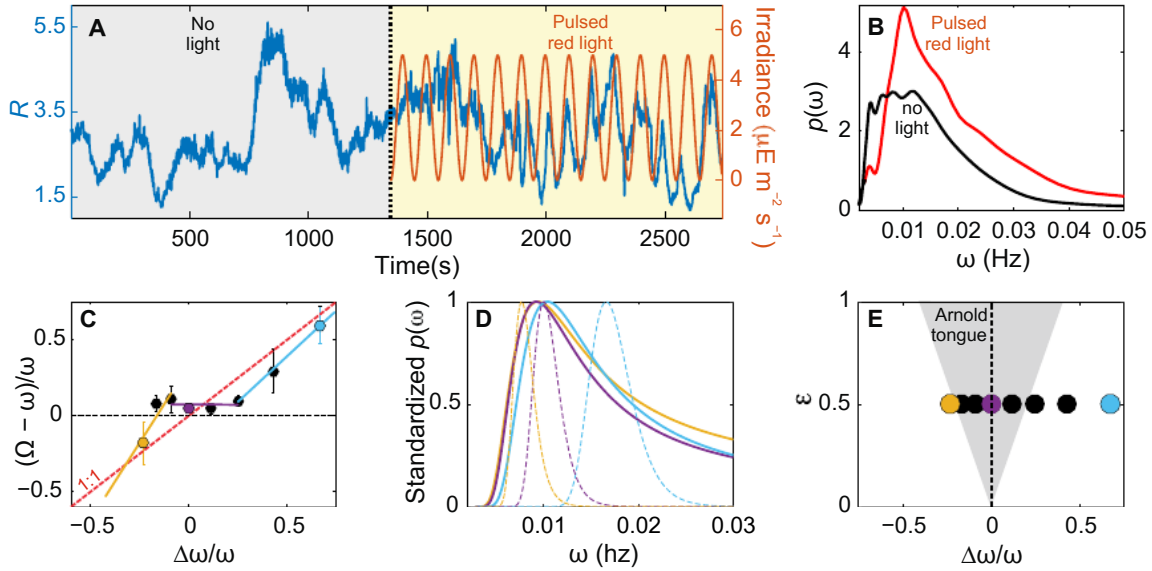

Fig. 3. Pulsed red light entrains cell wobbling frequency. (**A**) Temporal evolution of *P. delicatissima* population vertical alignment, as shown by *R* (*y* axis and blue line), displaying a progressive entrainment of cell wobbling frequency shortly after cells are exposed to pulsed red light of oscillating amplitude (secondary *y* axis on the right and orange line). (**B**) Power spectra for the measured wobbling signal with (red line) and without (in black) the forcing pulsed red light. (**C**) Emergent frequency difference between the wobble frequency (Ω) and pulsed red light-emitting diode (LED) light frequency (ω) (solid dots and continuous line) versus intrinsic frequency difference Δω between ω and the natural, unforced frequency of ~0.01 Hz (dashed line). (**D**) Power spectra for different ω. Solid lines correspond to the oscillation of *R* and dashed lines to the oscillation of red light. Colors correspond to values of ω depicted by solid dots of the same color in (C). (**E**) Illustration of the Arnold tongue. The potential for two oscillators to synchronize (gray area) is positively correlated with coupling strength and negatively correlated with the difference in intrinsic frequency. For fixed light intensity, a sweep in Δω is indicated as solid dots in the Arnold tongue diagram. Colors in (D) and (E) correspond to values of ω depicted by solid dots of the same color in (C).

Several consequences that deserve further exploration can be inferred from cell wobbling beyond communication. For example, since diatoms show distinct light transmission properties through their valves and gridle (*74*, *75*), wobbling provides a significant increase of light transmission through the frustule for wavelengths above 600 nm, modulating the light quality and quantity that reaches the interior of the cells and, more generally, the ocean light climate for others down the water column (*76*). We estimate that wobbling increases ~20% the direct solar radiation received by cells while sinking with a near-vertical orientation. Wobbling generates an unsteady sinking behavior that could increase the probability of cell-to-cell encounters, which is crucial for the sexual reproduction of pennate diatoms (*77*), reduces sinking speed (~20%), and increases nutrient uptake rates (*78*, *79*). Furthermore, the observed interaction between externally induced mechanical stresses (due to fluid mixing) and intracellular organization provides a new avenue for research on the sidelines of the more classical effects of mixing in nutrient gradients at the microscale (*80*). The above-described processes could thus strongly affect pennate diatom fitness and help understand their resilience in a changing ocean.

MATERIALS AND METHODS

Cell cultures

P. delicatissima

Cultures were maintained in sterile-filtered oligotrophic seawater amended with nutrients (K/2) at 17°C, under a 12:12 light/dark cycle and 80 μE m^{-2} s^{-1}, in algal incubators. The cultures were transferred once a week (dilution factor, ×8) to keep the cells healthy and in their exponential growth phase at maximum concentrations of ~10^8cell $liter^{-1}$. The cells rarely formed chains with more than 85% of the cultures composed of individual cells.

Experimental setup

Experiments were carried out in an in-house built setup for the concomitant measurement of particle size distribution and orientation, chlorophyll autofluorescence, and absorption spectra. The small volume (~100 ml) flow-through chamber from a LISST-100× laser diffractometer (Sequoia Scientific) was modified to incorporate an extra modulated (spectrally, via a monochromator, and in time) light line, orthogonal to the laser diffraction axis coupled to a power meter (PM16-130 from Thorlabs) and a Hamamatsu C12666MA mini-spectrometer as shown in fig. S1. This configuration allows for the interrogation of a wide range of experimental conditions and the simultaneous measurements of subsecond variations in cell orientation, light emission, and transmission.

Before each experiment, the LISST-100× chamber was precleaned and filled with the desired volume/volume concentration of cell culture (5×10^7 cells $liter^{-1}$). Agitation was induced by a 2-cm-long magnetic bar powered by the built-in speed controller of the chamber at minimum speed. Experiments consisted in an initial mixing phase where agitation was turned on (100 s), followed by a sedimentation phase where the system could evolve without any external disturbance. Separate experiments were performed with living cells, living cells with myosin adenosine triphosphatase inhibitor, BDM (*78*) and dead cells [killed by adding 1% (v/v) of Lugol's iodine solution]. Control experiments were carried out with culture medium without cells and with miliQ water.

Diatom response to light-dark cycles

To study the effect of light conditions on cell orientations, we carried out experiments in which periods of light and dark were alternated. During the light periods, the cells were illuminated with white light with an intensity of 10 μE m^{-2} s^{-1} for 45 min, followed by 45 min of complete darkness. This was repeated for >5 complete light-dark cycles.

Diatom response to pulsed red light

To study the response of *P. delicatissima* to pulsed red light, cells were illuminated by a 660-nm light-emitting diode (LED; M660L4-C, Thorlabs) through a neutral density filter (ND10A, Thorlabs) used to attenuate light intensity down to a maximum value of ~5μE m^{-2} s^{-1}. This intensity was then modulated sinusoidally with periods in a range slightly differing from cell wobbling natural frequency, i.e., from 60 to 130 s.

Fluorescence signal variations measurement

Variations in the cells' chlorophyll autofluorescence were measured by illuminating the culture with an excitation BL (470 nm at 1.25 mW) for 45 min while the cells settled without disturbance. The emitted red light coming from the cells was measured every second by the orthogonal power meter via a high-pass red filter (λ greater than 645 nm; FGL645M, Thorlabs).

Light absorption experiments

Light absorption experiments were carried out with a full light spectrum that shone, through a continuous filter monochromator (Zeiss 475808), into a suspension of 1.25×10^8 cells $liter^{-1}$ and measuring variations in the absorption spectra with an ultracompact mini-spectrophotometer at 10 distinct illumination wavelengths in the (400 to 700 nm) range. Measurements were taken for 20 min for the live and Lugol's iodine samples and 1 min for the control.

Laser diffractometry

LD measurements were used to obtain the particle volume concentration by size ranges (i.e., volume of particles in the seawater per unit volume of seawater) using a technique based on laser diffraction theory. The LISST-100X used in this study uses a 670-nm collimated laser beam to illuminate the suspended particles, and a 32-ring detector measures the intensity of the scattered light, corresponding to 32 different size classes logarithmically spaced. The angular pattern of optical scattering depends on the physical characteristics of the particles (e.g., size, shape, and orientation) and is used to calculate the particle volume concentration in these size classes (*81*). LD can be used to adequately characterize the different dimensions of nonspherical particles in specific orientations (*77*, *82*, *83*). Using this property, a method to infer the preferential orientation of particles in a suspension has been recently described (*84*). Here, we use this method to characterize the preferential orientation of diatoms under distinct physical conditions: LD measurements of nearly spheroidal cells are interpreted in terms of the relative variation of two size bands: from 2.72 to 3.78 μm (r_1) and from 14.65 to 33.4 μm (r_2), representing the known (measured from microscopy) major and minor cell axes (r_1 and r_2) of *P. delicatissima*. As cells orient in different directions, the signal in the size bands representing these axes presents an opposite behavior, with an inverse correlation between both groups ($r = -0.92$, $P < 0.001$) and direct correlation between sizes within the same size band ($r = 0.95$, $P < 0.001$). Hence, we can confidently compute the ratio between the signal from each of these two size bands, $R(t) = (\Sigma\, VD_1)/(\Sigma\, VD_2)$, as a scalar proxy for cell orientation (*77*, *84*). Phase space reconstruction of the R time series following Takens embedding theorem was analyzed using the PhaseRecurr MATLAB function (developed by J. Sorokin).

Particle image velocimetry

Measurements were performed using a commercial ultrabright LED pulsing particle image velocimetry (PIV) system (LED Pulsing System; iLA5150 GmbH), with polyamide particles as flow tracers (mean diameter of 57 μm and density of 1.016 $g{\cdot}cm^{-3}$), a 5-MP uEye IDS complementary metal-oxide semiconductor (CMOS) camera with a 35-mm lens set at a 20-cm working distance and double 100-μs-long green light pulses shifted 2 ms (overall period set to 10 frames per second). The LISST-100× small-volume flow-through chamber was precleaned and filled with a 200 μl per 100 ml (v/v) microbead solution in Milli-Q water. PIV multipass correlations analysis was run with three iterative steps and a minimum of 16 × 16 pixels window size. For long time series experiments, the extracted instantaneous velocity fields were further running-averaged over 1-s intervals to evaluate the mean shear rate.

Measurements of chloroplast arrangement

The effect of light on the arrangement of chloroplasts in cells was studied using a particle scanning and imaging system. Samples were processed with a pulse shape flow cytometer equipped with an inflow imaging system (Cytosense from Cytobuoy). Self-organizing maps (SOMs) (*85*) of the fluorescence signal were used to identify the subtle changes in the chloroplast arrangement of 20,000 cells. From a cluster of individual cell images and, after standardization of cell length, the arrangement of chloroplasts was analyzed. The positions of the chloroplasts of 10,000 cells exposed to daylight (of the same intensity as the LD experiments) and that of 10,000 cells that were under dark conditions were recorded and analyzed. Figure S5A shows the 25 characteristic patterns in which the SOM classified the set of data. These patterns are grouped in the figure by degree of similarity so that the most similar patterns are found in adjacent positions, while the most distinct patterns are found in the corners. Each of these is representative of a set of cells; in fig. S5B, it is shown whether these patterns are dominant in light (positive values) or dark (negative values) conditions.

Sinking cell model with variable CoM

The dynamics of sinking ellipsoids was integrated following (*86*), and it is solely based on a balance of viscous and gravitational torques in the Stokes flow regime. Any organelle displacement causing a deviation from a precise symmetric mass density distribution within a cell has to induce a shift in the position of the CoM. We have further incorporated these shifts into the model to account for an oscillatory dynamics for the position of the CoM with period and amplitude (~30° maximum angular displacements) extracted from our experimental data.

SUPPLEMENTARY MATERIALS

Supplementary material for this article is available at https://science.org/doi/10.1126/sciadv.abj5230

REFERENCES AND NOTES

1. J. M. Henke, B. L. Bassler, Bacterial social engagements. *Trends Cell Biol.* **14**, 648–656 (2004).
2. J. W. Jolles, A. J. King, S. S. Killen, The role of individual heterogeneity in collective animal behaviour. *Trends Ecol. Evol.* **35**, 278–291 (2020).

3. D. J. T. Sumpter, The principles of collective animal behaviour. *Philos. Trans. R. Soc. B Biol. Sci.* **361**, 5–22 (2006).
4. N. Marquet, C. Conand, D. M. Power, A. V. M. Canário, M. González-Wangüemert, Sea cucumbers, *Holothuria arguinensis* and *H. mammata*, from the southern Iberian Peninsula: Variation in reproductive activity between populations from different habitats. *Fish. Res.* **191**, 120–130 (2017).
5. M. Iacchei, T. Ben-Horin, K. A. Selkoe, C. E. Bird, F. J. García-Rodríguez, R. J. Toonen, Combined analyses of kinship and FST suggest potential drivers of chaotic genetic patchiness in high gene-flow populations. *Mol. Ecol.* **22**, 3476–3494 (2013).
6. S. DeWeerdt, Sea change. *Nature* **550**, S54–S58 (2017).
7. B. J. Crespi, The evolution of social behavior in microorganisms. *Trends Ecol. Evol.* **16**, 178–183 (2001).
8. A. Vardi, D. Schatz, K. Beeri, U. Motro, A. Sukenik, A. Levine, A. Kaplan, Dinoflagellate-cyanobacterium communication may determine the composition of phytoplankton assemblage in a mesotrophic lake. *Curr. Biol.* **12**, 1767–1772 (2002).
9. G. Parker, Y. Akamatsu, W. Dietrich, in *Proceedings, International Conference on Civil and Environmental Engineering (ICCEE-2004), Hiroshima University, Japan, 27 to 28 July 2004* (Department of Social and Environmental Engineering, Hiroshima University, 2004), pp. 1–10.
10. J. D. Long, G. W. Smalley, T. Barsby, J. T. Anderson, M. E. Hay, Chemical cues induce consumer-specific defenses in a bloom-forming marine phytoplankton. *Proc. Natl. Acad. Sci.* **104**, 10512–10517 (2007).
11. S. Schauder, B. L. Bassler, The languages of bacteria. *Genes Dev.* **15**, 1468–1480 (2001).
12. M. E. Taga, B. L. Bassler, Chemical communication among bacteria. *Proc. Natl. Acad. Sci.* **100**, 14549–14554 (2003).
13. S. Schulz, A new bacterial chemical signal: Mapping the chemical space used for communication. *Chembiochem* **15**, 498–500 (2014).
14. M. E. Hay, Marine chemical ecology: Chemical signals and cues structure marine populations, communities, and ecosystems. *Annu. Rev. Mar. Sci.* **1**, 193–212 (2009).
15. L. Labeeuw, A. R. Bramucci, R. J. Case, in *Systems Biology of Marine Ecosystems* (Springer, 2017), pp. 279–300.
16. G. Pohnert, M. Steinke, R. Tollrian, Chemical cues, defence metabolites and the shaping of pelagic interspecific interactions. *Trends Ecol. Evol.* **22**, 198–204 (2007).
17. A. Ianora, G. Romano, Y. Carotenuto, F. Esposito, V. Roncalli, I. Buttino, A. Miralto, Impact of the diatom oxylipin 15S-HEPE on the reproductive success of the copepod *Temora stylifera*. *Hydrobiologia* **666**, 265–275 (2011).
18. E. Van Donk, A. Ianora, M. Vos, Induced defences in marine and freshwater phytoplankton: A review. *Hydrobiologia* **668**, 3–19 (2011).
19. K. E. Whalen, C. Kirby, R. M. Nicholson, M. O'Reilly, B. S. Moore, E. L. Harvey, The chemical cue tetrabromopyrrole induces rapid cellular stress and mortality in phytoplankton. *Sci. Rep.* **8**, 15498 (2018).
20. E. Selander, J. Kubanek, M. Hamberg, M. X. Andersson, G. Cervin, H. Pavia, Predator lipids induce paralytic shellfish toxins in bloom-forming algae. *Proc. Natl. Acad. Sci.* **112**, 6395–6400 (2015).
21. E. A. Widder, Bioluminescence in the ocean: Origins of biological, chemical, and ecological diversity. *Science* **328**, 704–708 (2010).
22. K. H. Nealson, J. W. Hastings, Bacterial bioluminescence: Its control and ecological significance. *Microbiol. Rev.* **43**, 496–518 (1979).
23. E. V. Armbrust, The life of diatoms in the world's oceans. *Nature* **459**, 185–192 (2009).
24. C. B. Field, Primary production of the biosphere: Integrating terrestrial and oceanic components. *Science* **281**, 237–240 (1998).
25. P. G. Falkowski, R. T. Barber, V. Smetacek, Biogeochemical controls and feedbacks on ocean primary production. *Science* **281**, 200–207 (1998).
26. G. Sarthou, K. R. Timmermans, S. Blain, P. Tréguer, Growth physiology and fate of diatoms in the ocean: A review. *J. Sea Res.* **53**, 25–42 (2005).
27. A. Falciatore, M. R. d'Alcalà, P. Croot, C. Bowler, Perception of environmental signals by a marine diatom. *Science* **288**, 2363–2366 (2000).
28. K. G. V Bondoc, J. Heuschele, J. Gillard, W. Vyverman, G. Pohnert, Selective silicate-directed motility in diatoms. *Nat. Commun.* **7**, 10540 (2016).
29. A. Vardi, F. Formiggini, R. Casotti, A. De Martino, F. Ribalet, A. Miralto, C. Bowler, A stress surveillance system based on calcium and nitric oxide in marine diatoms. *PLoS Biol.* **4**, e60 (2006).
30. J. Sai, C. H. Johnson, Dark-stimulated calcium ion fluxes in the chloroplast stroma and cytosol. *Plant Cell* **14**, 1279–1291 (2002).
31. M. J. J. Huysman, W. Vyverman, L. De Veylder, Molecular regulation of the diatom cell cycle. *J. Exp. Bot.* **65**, 2573–2584 (2014).
32. P. R. F. Rocha, A. D. Silva, L. Godinho, W. Dane, P. Estrela, K. J. Vandamme, J. B. Pereira-leal, D. M. De Leeuw, R. B. Leite, Collective electrical oscillations of a diatom population induced by dark stress. *Sci. Rep.* **8**, 5484 (2018).
33. A. Vardi, Cell signaling in marine diatoms. *Commun. Integr. Biol.* **1**, 134–136 (2008).
34. T. Kadono, A. Miyagawa-Yamaguchi, N. Kira, Y. Tomaru, T. Okami, T. Yoshimatsu, L. Hou, T. Ohama, K. Fukunaga, M. Okauchi, H. Yamaguchi, K. Ohnishi, A. Falciatore, M. Adachi, Characterization of marine diatom-infecting virus promoters in the model diatom *Phaeodactylum tricornutum*. *Sci. Rep.* **5**, 18708 (2015).
35. F. Takahashi, Blue-light-regulated transcription factor, Aureochrome, in photosynthetic stramenopiles. *J. Plant Res.* **129**, 189–197 (2016).
36. K. Wirtz, S. L. Smith, Vertical migration by bulk phytoplankton sustains biodiversity and nutrient input to the surface ocean. *Sci. Rep.* **10**, 1–12 (2020).
37. A. R. Nayak, M. N. McFarland, J. M. Sullivan, M. S. Twardowski, Evidence for ubiquitous preferential particle orientation in representative oceanic shear flows. *Limnol. Oceanogr.* **63**, 122–143 (2018).
38. R. C. Perez, G. R. Foltz, R. Lumpkin, C. Schmid, Direct measurements of upper ocean horizontal velocity and vertical shear in the tropical North Atlantic at 4 N, 23 W. *J. Geophys. Res. Ocean* **124**, 4133–4151 (2019).
39. B. Lepetit, R. Goss, T. Jakob, C. Wilhelm, Molecular dynamics of the diatom thylakoid membrane under different light conditions. *Photosynth. Res.* **111**, 245–257 (2012).
40. W. Krzeszowiec, B. Rajwa, J. Dobrucki, H. Gabryś, Actin cytoskeleton in *Arabidopsis thaliana* under blue and red light. *Biol. Cell.* **99**, 251–260 (2007).
41. Y. Sakai, S. Takagi, Roles of actin cytoskeleton for regulation of chloroplast anchoring. *Plant Signal. Behav.* **12**, e1370163 (2017).
42. T. Furukawa, M. Watanabe, I. Shihira, Green- and blue-light-mediated chloroplast migration in the centric diatom *Pleurosira laevis*. *Protoplasma* **203**, 214–220 (1998).
43. S.-T. Chen, C.-W. Li, Relationships between the movements of chloroplasts and cytoskeletons in diatoms. *Bot. Mar.* **34**, 505–512 (1991).
44. L. A. Edgar, M. Zavortink, The mechanism of diatom locomotion. II. Identification of actin. *Proc. R. Soc. Lond. Ser. B Biol. Sci.* **218**, 345–348 (1983).
45. N. C. Poulsen, I. Spector, T. P. Spurck, T. F. Schultz, R. Wetherbee, Diatom gliding is the result of an actin-myosin motility system. *Cell Motil. Cytoskeleton* **44**, 23–33 (1999).
46. I. Shihira-Ishikawa, T. Nakamura, S. Higashi, M. Watanabe, Distinct responses of chloroplasts to blue and green laser microbeam irradiations in the centric diatom *Pleurosira laevis*. *Photochem. Photobiol.* **83**, 1101–1109 (2007).
47. Y. Sato, M. Wada, A. Kadota, Choice of tracks, microtubules and/or actin filaments for chloroplast photo-movement is differentially controlled by phytochrome and a blue light receptor. *J. Cell Sci.* **114**, 269–279 (2001).
48. S. Takagi, Actin-based photo-orientation movement of chloroplasts in plant cells. *J. Exp. Biol.* **206**, 1963–1969 (2003).
49. H. Paves, E. Truve, Myosin inhibitors block accumulation movement of chloroplasts in *Arabidopsis thaliana* leaf cells. *Protoplasma* **230**, 165–169 (2007).
50. E. De Tommasi, I. Rendina, I. Rea, M. De Stefano, A. Lamberti, L. De Stefano, *Optical Sensors 2009* (International Society for Optics and Photonics, 2009), vol. 7356, p. 735615.
51. N. Mazumder, A. Gogoi, R. D. Kalita, G. A. Ahmed, A. K. Buragohain, A. Choudhury, Luminescence studies of fresh water diatom frustules. *Indian J. Phys.* **84**, 665–669 (2010).
52. G. Di Caprio, G. Coppola, L. De Stefano, M. De Stefano, A. Antonucci, R. Congestri, E. De Tommasi, Shedding light on diatom photonics by means of digital holography. *J. Biophotonics* **7**, 341–350 (2014).
53. P. LeDuff, G. Roesijadi, G. L. Rorrer, Micro-photoluminescence of single living diatom cells. *Luminescence* **31**, 1379–1383 (2016).
54. K. Kieu, C. Li, Y. Fang, G. Cohoon, O. D. Herrera, M. Hildebrand, K. H. Sandhage, R. A. Norwood, Structure-based optical filtering by the silica microshell of the centric marine diatom *Coscinodiscus wailesii*. *Opt. Express* **22**, 15992–15999 (2014).
55. M. Ghobara, N. Mazumder, V. Vinayak, L. Reissig, I. C. Gebeshuber, M. A. Tiffany, R. Gordon, On light and diatoms: A photonics and photobiology review, in *Diatoms: Fundamentals and Application* (Wiley, 2019), pp. 129–189.
56. C. D. Mobley, C. D. Mobley, *Light and Water: Radiative Transfer in Natural Waters* (Academic Press, 1994).
57. M. Ragni, M. Ribera D'Alcalà, Light as an information carrier underwater. *J. Plankton Res.* **26**, 433–443 (2004).
58. P. G. Falkowski, J. A. Raven, *Aquatic Photosynthesis* (Princeton Univ. Press, 2013).
59. K. Maxwell, G. N. Johnson, Chlorophyll fluorescence—A practical guide. *J. Exp. Bot.* **51**, 659–668 (2000).
60. W. Hillier, G. T. Babcock, Photosynthetic reaction centers. *Plant Physiol.* **125**, 33–37 (2001).
61. S. R. Laney, R. M. Letelier, R. A. Desiderio, M. R. Abbott, D. A. Kiefer, C. R. Booth, Measuring the natural fluorescence of phytoplankton cultures. *J. Atmos. Ocean. Technol.* **18**, 1924–1934 (2001).
62. J. Romann, J.-C. Valmalette, M. S. Chauton, G. Tranell, M.-A. Einarsrud, O. Vadstein, Wavelength and orientation dependent capture of light by diatom frustule nanostructures. *Sci. Rep.* **5**, 17403 (2015).
63. F. A. Depauw, A. Rogato, M. Ribera d'Alcalá, A. Falciatore, Exploring the molecular basis of responses to light in marine diatoms. *J. Exp. Bot.* **63**, 1575–1591 (2012).
64. S. König, M. Juhas, S. Jäger, T. Kottke, C. Büchel, The cryptochrome—Photolyase protein family in diatoms. *J. Plant Physiol.* **217**, 15–19 (2017).

65. B. Schellenberger Costa, A. Jungandreas, T. Jakob, W. Weisheit, M. Mittag, C. Wilhelm, Blue light is essential for high light acclimation and photoprotection in the diatom *Phaeodactylum tricornutum*. *J. Exp. Bot.* **64**, 483–493 (2013).
66. A. E. Fortunato, M. Jaubert, G. Enomoto, J.-P. Bouly, R. Raniello, M. Thaler, S. Malviya, J. S. Bernardes, F. Rappaport, B. Gentili, Diatom phytochromes reveal the existence of far-red-light-based sensing in the ocean. *Plant Cell* **28**, 616–628 (2016).
67. F. A. Depauw, Light perception in marine diatoms and characterization of a novel phytochrome from *Phaeodactylum tricornutum*, thesis, The Open University (2014).
68. C. Leblanc, A. Falciatore, M. Watanabe, C. Bowler, Semi-quantitative RT-PCR analysis of photoregulated gene expression in marine diatoms. *Plant Mol. Biol.* **40**, 1031–1044 (1999).
69. S. Coesel, M. Oborník, J. Varela, A. Falciatore, C. Bowler, Evolutionary origins and functions of the carotenoid biosynthetic pathway in marine diatoms. *PLOS ONE* **3**, e2896 (2008).
70. M. Jaubert, J.-P. Bouly, M. R. d'Alcalà, A. Falciatore, Light sensing and responses in marine microalgae. *Curr. Opin. Plant Biol.* **37**, 70–77 (2017).
71. A. S. Pikovsky, M. Rosenblum, J. Kurths, Synchronization—A unified approach to nonlinear science. *Phys. Today* **56**, 47 (2010).
72. A. E. Fisher, J. A. Berges, P. J. Harrison, Does light quality affect the sinking rates of marine diatoms? 1. *J. Phycol.* **32**, 353–360 (1996).
73. J.-L. Mouget, R. Gastineau, O. Davidovich, P. Gaudin, N. A. Davidovich, Light is a key factor in triggering sexual reproduction in the pennate diatom *Haslea ostrearia*. *FEMS Microbiol. Ecol.* **69**, 194–201 (2009).
74. J. W. Goessling, Y. Su, P. Cartaxana, C. Maibohm, L. F. Rickelt, E. C. L. Trampe, S. L. Walby, D. Wangpraseurt, X. Wu, M. Ellegaard, M. Kühl, Structure-based optics of centric diatom frustules: Modulation of the in vivo light field for efficient diatom photosynthesis. *New Phytol.* **219**, 122–134 (2018).
75. J. W. Goessling, Biophotonics of diatoms: Linking frustule structure to photobiology, thesis, University of Copenhagen (2017).
76. J. Marcos, R. Seymour, M. Luhar, W. M. Durham, J. G. Mitchell, A. Macke, R. Stocker, Microbial alignment in flow changes ocean light climate. *Proc. Natl. Acad. Sci. U.S.A.* **108**, 3860–3864 (2011).
77. J. S. Font-Muñoz, R. Jeanneret, J. Arrieta, S. Anglès, A. Jordi, I. Tuval, G. Basterretxea, Collective sinking promotes selective cell pairing in planktonic pennate diatoms. *Proc. Natl. Acad. Sci. U.S.A.* **116**, 15997–16002 (2019).
78. B. J. Gemmell, G. Oh, E. J. Buskey, T. A. Villareal, Dynamic sinking behaviour in marine phytoplankton: Rapid changes in buoyancy may aid in nutrient uptake. *Proc. Biol. Sci.* **283**, 20161126 (2016).
79. K. T. Du Clos, L. Karp-Boss, B. J. Gemmell, Diatoms rapidly alter sinking behavior in response to changing nutrient concentrations. *Limnol. Oceanogr.* **66**, 892–900 (2021).
80. L. Karp-Boss, E. Boss, P. A. Jumars, Nutrient fluxes to planktonic osmotrophs in the presence of fluid motion. *Oceanogr. Mar. Biol.* **34**, 71–107 (1996).
81. Y. C. Agrawal, A. Whitmire, O. A. Mikkelsen, H. C. Pottsmith, Light scattering by random shaped particles and consequences on measuring suspended sediments by laser diffraction. *J. Geophys. Res. Ocean* **113**, C04023 (2008).
82. G. W. Graham, E. J. Davies, W. A. M. Nimmo-Smith, D. G. Bowers, K. M. Braithwaite, Interpreting LISST-100X measurements of particles with complex shape using digital in-line holography. *J. Geophys. Res. Ocean* **117**, C05034 (2012).
83. L. Karp-Boss, L. Azevedo, E. Boss, LISST-100 measurements of phytoplankton size distribution: Evaluation of the effects of cell shape. *Limnol. Oceanogr. Methods* **5**, 396–406 (2007).
84. J. S. Font-Muñoz, R. Jeanneret, I. Tuval, G. Basterretxea, Method for the determination of preferential orientation of marine particles from laser diffraction measurements. *Opt. Express* **28**, 14085–14099 (2020).
85. T. Kohonen, Analysis of a simple self-organizing process. *Biol. Cybern.* **44**, 135–140 (1982).
86. T. J. Pedley, J. O. Kessler, The orientation of spheroidal microorganisms swimming in a flow field. *Proc. R. Soc. Lond. B* **231**, 47–70 (1987).

Acknowledgments

Funding: This research was supported by ISblue project, Interdisciplinary graduate school for the Blue Planet (ANR-17-EURE-0015), and cofunded by a grant from the French government under the program "Investissements d'Avenir" and a grant from the Regional Council of Brittany (SAD program); additional funding from grants CTM2017-83774-P, PID2019-104232GB-I00, PD/018/2020, and IED2019-000958-I from the Spanish Ministerio de Ciencia e Innovación (MICINN), the Agencia Estatal de Investigación (AEI), the Margalida Comas Program, the Fondo Europeo de Desarrollo Regional (FEDER, UE), Interreg Atlantic Area Programme Project PRIMROSE (EAPA_182/2016). **Author contributions:** Conceptualization: J.S.F.-M., M.S., I.T., and G.B. Formal analysis: J.S.F.-M. and I.T. Methodology: J.S.F.-M., I.T., M.S., and A.C.-S. Investigation: J.S.F.-M., M.S., I.T., and A.C.-S. Visualization: I.T. and G.B. Funding acquisition: J.S.F.-M., M.S., I.T., and G.B. Project administration: J.S.F.-M. Writing (original draft): J.S.F.-M., I.T., and G.B. Writing (review and editing): J.S.F.-M., M.S., I.T., and G.B. **Competing interests:** The authors declare that they have no competing interests **Data and materials availability:** All data needed to evaluate the conclusions in the paper are present in the paper and/or the Supplementary Materials.

Submitted 18 May 2021
Accepted 27 October 2021
Published 15 December 2021
10.1126/sciadv.abj5230